

Galaxy destruction and diffuse light in clusters

Carlos Calcáneo-Roldán¹★, Ben Moore¹, Joss Bland-Hawthorn², David Malin²
and Elaine M. Sadler.³

¹Department of Physics, University of Durham, Durham DH1 3LE, UK.

²Anglo-Australian Observatory, Epping Laboratory, P.O. BOX 296, Epping NSW.

³University of Sydney, School of Physics, Sydney NSW 2006, Australia.

August 1998

ABSTRACT

Deep images of the Centaurus and Coma clusters reveal two spectacular arcs of diffuse light that stretch for over 100 kpc, yet are just a few kpc wide. At a surface brightness of $m_b \sim 27 - 28$ th arcsec $^{-2}$, the Centaurus arc is the most striking example known of structure in the diffuse light component of a rich galaxy cluster. We use numerical simulations to show that this feature is most probably the tidal debris of a low surface brightness (LSB) disk galaxy that has been disrupted by galaxy harassment, primarily by the gravitational potential of NGC 4709. High surface brightness disk galaxies are more stable to tidal shocks and lose less stellar mass, therefore their tidal debris is significantly fainter. Spheroidal galaxies can also produce features in the diffuse light component, yet these are even more diffuse and not as narrow. Only a luminous LSB galaxy on a fairly radial orbit, whose disk is co-rotating with its orbital path past pericentre can provide an acceptable reproduction of the extent, width and brightness of the Centaurus arc. Features this prominent in clusters will be relatively rare, although at fainter surface brightness levels the diffuse light will reveal a wealth of structure. Deeper imaging surveys may be able to trace this feature for several times its presently observed extent and somewhere along the tidal debris, a fraction of the original stellar component of the disk will remain bound, but transformed into a faint spheroidal galaxy. It should be possible to confirm the galactic origin of the Centaurus arc by observing planetary nebulae along its length with redshifts close to that of NGC 4709.

Key words: galaxies: evolution – galaxies: clusters – galaxies: interactions – galaxies: formation.

1 INTRODUCTION

Detecting diffuse light in clusters has an enigmatic history spanning several decades (de Vaucouleurs, 1960; Frei *et al* 1994; Thuan & Kormendy 1977; Uson *et al* 1991; Vilchez-Gómez *et al* 1994; Bernstein *et al* 1995; Tyson *et al* 1995). Using either CCDs or photographic imaging, these observations have been plagued by background subtraction, stray light within the telescope and optics, and atmospheric scattering. This has made a quantitative analysis difficult: the total amount of diffuse light, its colour, or its radial distribution have not yet been accurately measured. These techniques have lead to claims that as much as 70% of the light attached to galaxies may lie in a diffuse component. More

recently, individual planetary nebulae have been detected, inbetween cluster galaxies and with redshifts and velocities that place them inside the cluster potential (Arnaboldi *et al* 1996; Theuns & Warren 1996; Feldmeier *et al* 1997). Deep HST images of the Virgo cluster have also revealed a large population of freely orbiting, red-giant stars (Ferguson, Tanvir & Hippe 1997). These studies also indicate large quantities of diffuse light exist in clusters.

Intra-galactic stars must have formed within galaxies and have been subsequently ripped out by gravitational tidal forces – galaxy harassment (Moore *et al* 1996). Mergers do not occur within virialised clusters (Ghigna *et al* 1997), but the impulsive and resonant shocks from rapid fly-by encounters between galaxies can create tidal debris. In the absence of further perturbations, stars that are tidally removed from galaxies will orbit in narrow streams that trace the orbital

★ Email:C.A.Calcaneo-Roldan@durham.ac.uk

path of the galaxy. In a cluster, the star streams will be subsequently heated and mixed on a time-scale of a few crossing times, *i.e.* several billion years. We might therefore expect to find prominent features in the intra-cluster light component from recently disrupted galaxies that have accreted into clusters a few billion years ago.

The properties of the diffuse light, including its quantity, radial distribution, clumpiness and colour, are of great interest for many reasons. As well as constraining the importance of gravitational interactions as a mechanism for morphological transformation, we have the possibility of using thousands of freely orbiting stars for studying the cluster potential. Understanding the orbital biases of stripped stars and their subsequent evolution within a clumpy potential, will be vital in the interpretation of these velocity data.

Recently, Trentham & Mobasher (1997) detected a low surface brightness feature ~ 80 kpc long within the Coma cluster, that may be the result of a high speed encounter between two galaxies. Conselice & Gallagher (1998) also find a wealth of fine scale substructure and faint tidal features in a survey of several nearby clusters. Here we “re-discover” a much more spectacular arc of diffuse light that stretches for over 100 kpc near NGC4709 within the Centaurus cluster. The stacked sequence of photographic images by David Malin were first reported very briefly in the Anglo-Australian newsletter by John Lucey over 16 years ago; no further attention has since been given to these data. Using the same techniques we have also discovered a second feature that lies near the centre of the Coma cluster that is morphologically similar to the Centaurus arc.

Although the “galaxy harassment” simulations of Moore *et al* (1996) predicted that clusters should contain a wealth of structure at very low surface brightness levels, $m_b \gtrsim 29$ th arcsec $^{-2}$, their simulations were focused on the evolution of fainter Sc-Sd galaxies in clusters. Could prominent features such as the Centaurus arc arise from the debris of a disrupted L* spiral? With only a couple of documented examples, why are prominent features as bright as these so rare? One possibility is that the diffuse light in clusters arises from a population of low surface brightness (LSB) spiral galaxies that are destroyed by tidal forces once they enter the cluster environment. These features in the diffuse light component may be the “smoking gun” from recent accretions of LSB spiral’s into clusters.

This paper is organized as follows. Section 2 discusses the properties of the two newly discovered arcs, including photographic and CCD colour information of the Centaurus arc, ending with a discussion of alternative mechanisms to “harassment” for the origin of these features. Section 3 begins with a description of the numerical techniques and galaxy models that we shall use, and follows with a detailed attempt to reproduce the gross properties of the arc by disrupting galaxies of different morphologies within a cluster potential. In Section 4 we discuss the most likely origin for the Centaurus arc, discriminating between the different models. Our results are concluded in Section 5.

2 THE IMAGES

The Centaurus arc was originally discovered by applying a photographic amplification technique (Malin 1978) to three

plates taken by Malcolm Smith at the f/2.66 prime focus of the 4m telescope of the Cerro Tololo Inter-American observatory (CTIO, 1974). The photographic emulsion was Eastman Kodak type IIIaJ, hyper-sensitized by baking in nitrogen before use. Photographically amplified positive derivatives from these plates were combined into one image (Malin 1981) to improve the image quality and minimize processing non-uniformities. The arc was clearly visible on each of the three copies, and its reality was latter confirmed by photographic amplification of IIIaJ plates taken with the 3.9 m Anglo-Australian Telescope and the 1.2 m UK Schmidt telescope.

More recent CCD observations reveal that if this structure lies in the cluster, it is $\sim 120 h^{-1}$ kpc (~ 12 arcmin) long and only $1 - 2 h^{-1}$ kpc ($\sim 10 - 15$ arcsec) wide (Throughout this paper $H_0 = 100 h \text{Mpc km s}^{-1}$, $h = 1$). The arc has very low surface brightness ($\mu_B \gtrsim 27.8$ mag arcsec $^{-2}$), is red in colour and points towards the active elliptical galaxy NGC4696. The arc’s colour strongly suggests that it is made of stars, so its narrowness is remarkable. The arc is not perfectly straight and has a small curvature along its length.

The top half of Figure 1 shows a negative print of part of the photographically amplified, combined images of the CTIO plates. The arc is the linear feature that extends from the lower left corner (south east) towards the nucleus of NGC4696. The lower image shows the same part of the sky on a single unamplified plate.

The photographs (and CCD frames) show the arc to be diffuse and seemingly devoid of fine structure at the arcsec level. While there are many faint stars and galaxies in the field, there is no apparent enhancement of point-like or diffuse objects along its length. (The point-like source near the centre of the arc is a star). The arc first becomes visible near a small, edge-on S0 galaxy, ESO 322-G102, at a projected distance of about $80 h^{-1}$ kpc from NCG 4696; the truncation of the arc at this point may be a line-of-sight coincidence, since there is no evidence of any interaction between the arc and ESO 322-G102. Subtraction of the extended light profile of NGC 4696 may reveal the arc on the opposite side of the S0 galaxy.

Spectroscopy of the arc would be extremely difficult in view of its very low surface brightness, however, broadband CCD images of the brightest regions were obtained making it possible to compare the colours of the arc with aged stellar populations. CCD pictures were taken in B, R and I bands with an RCA 350x512 chip at the f/3.3 prime focus of the AAT under photometric conditions on the night of 21/22 June 1990. The CCD scale was 0.49 arcsec/pixel, and the seeing 2 – 3 arcsec. Two sets of overlapping exposures were taken, with total exposure times of 90 minutes in B, 40 minutes in R and 20 minutes in I. Flat fields and bias frames were taken on the same night.

Table 1 lists the surface brightness and colours of the arc as measured from the overlap region of the CCD frames. In each case, the mean surface brightness in three regions along the arc was measured, each roughly 5×5 arcsec 2 and free of obvious foreground stars, and six ‘sky’ regions of similar area straddling the arc and just outside it. The errors quoted in Table 1 are 1σ errors on the mean of the three sky-subtracted arc measurements in each filter.

The CCD measurements confirm that the arc is extremely diffuse and very faint, reaching no more than 0.7%

See fig1.jpg

Surface brightness (mag arcsec ⁻²)	Colour (mag)
Arc	
$\mu_B = 27.81 \pm 0.08$	$B - R = +1.72 \pm 0.13$
$\mu_R = 26.09 \pm 0.05$	$R - I = +0.35 \pm 0.22$
$\mu_I = 25.74 \pm 0.17$	
Sky (I frame in twilight)	
$\mu_B = 22.52$	
$\mu_R = 20.76$	
$\mu_I = 18.78$	

See fig2.jpg

Table 1. Surface brightness and colours of the arc and sky.

of the brightness of the night sky. Further out, the arc is even fainter and we estimate that the faintest parts of the structure revealed by the photographic plates are only 0.1% of the night sky brightness.

The same techniques have also been applied to photographic images of the central regions of the Coma cluster (Abell 1656). These have revealed a feature in the diffuse light, close to NGC 4874, that stretches East-West for at least 5 arcmin, $\sim 150 h^{-1}$ kpc (Figure 2). It is curved slightly concave to NGC 4874 in a manner very similar to the curve in the Centaurus cluster feature where it appears closest to NGC 4709. The image was made by combining photographically amplified derivatives from three UK Schmidt plates. Two of the plates (J9946 and J10027) were deep IIIa-J (395-550nm) exposures while one was plate OR9945 covering the range 590-700nm. The linear feature is visible individually on all of the plates, but is much less obvious on the red-light plate. Given the large airmass through which the exposures were necessarily made and the smaller number of plates, this suggests that the surface brightness of the Coma arc is higher than that in the Centaurus cluster. The large airmass has also contributed to the relatively poor seeing in these plates, which is probably why we are unable to confirm the Trentham & Mobasher (1997) feature.

The arc is neither as narrow nor as well defined as that in the Centaurus cluster and two resolved galaxies appear to be embedded in the brightest part of it. Given the large number of galaxies in the field, this could be a line-of-sight coincidence, or one of these could be the remnant nucleus of a disrupted galaxy. In the absence of CCD photometry of the Coma arc, and its poorer resolution due to its distance, we shall focus our attention at the Centaurus arc.

2.1 Possible origins

The Centaurus arc is unlikely to be foreground reflection nebulosity in our own Galaxy. Malin has used his photographic amplifications technique on many fields containing Galactic nebulosity, and notes that the Centaurus feature (at Galactic latitude 22°) is morphologically quite different. In particular, it lacks the high-frequency ‘crumpling’ characteristic of Galactic cirrus and reflection nebulosity. Also, the arc is almost straight (it deviates from a straight line by at most 3–4 arcsec in the 100 arcsec length covered by the CCD frames) and points at the nucleus of NGC 4696, the brightest galaxy in the Centaurus cluster.

Figure 2. A high-contrast image of the core of the Coma galaxy cluster with NGC 4874 at the upper right. One arcmin at the distance of Coma is approximately $30 h^{-1}$ kpc.

The region of the arc observed with the CCD has colours consistent with those of K0 stars in the (B-R), (R-I) two-colour diagram (Figure 3, Cousins 1981). If the arc were dominated by optical synchrotron radiation it would be bluer than this, with B-R around 0.7-1.2 as typically seen in BL Lac objects (Moles *et al* 1985) and the M87 jet (Tarenghi 1981). Whilst the arc might be composed of ionized gas, with most of its light coming from O⁺⁺ and H⁺ ions, very unusual line ratios would be needed to produce the observed colours and it would be difficult to account for the I-band emission. Furthermore, it is hard to imagine a long-lived ionizing source which could operate over such a large distance. If light from the arc originated from emission lines, we would also need to account for the collimation of the ionized gas, or the ionizing beam, or both. We therefore conclude that the arc is probably composed of stars with a mean spectral class of around K0.

Could the feature be a gravitational arc from a background galaxy that has been lensed by the combined potential of NGC4696 and NGC4709? In order to produce a gravitationally lensed image this straight, the potential has to be complex, such as would occur in between the combined potential of the two central cDs. Furthermore, a lensed image this close to the massive potential of NGC4709, would produce a much shorter image. Thus, its position and morphology rule out gravitational lensing.

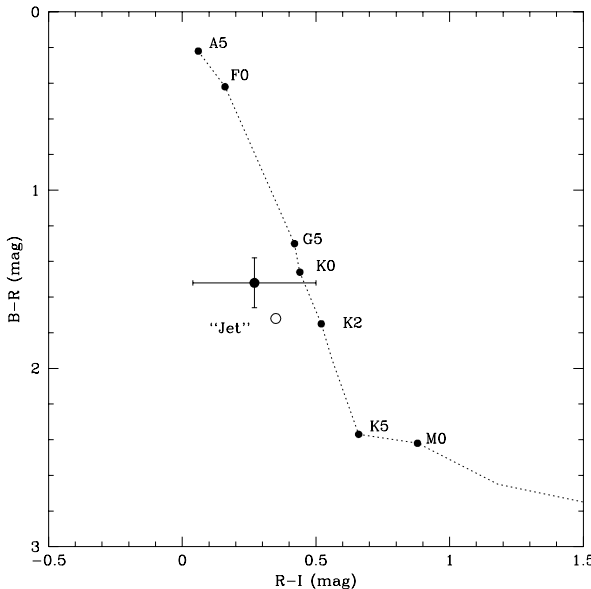


Figure 3. The Colours of the Centaurus arc compared with those of late-type giant stars. The solid circle is the reddening corrected value, the open circle is the value without this correction.

The dimensions of the object rule out a diffuse galaxy that happens to lie along the line of sight - the axial ratios are about sixty to one. If the Centaurus arc is stellar and lies in the cluster, then either the stars formed *in situ*, or they have been removed from one of the cluster galaxies; since no mechanism is known for the former, we shall concentrate on the latter. In either case, the key challenge for any successful model for its origin is to reproduce both the length and narrowness of the feature.

We can estimate the mass of the stars in the arc from its integrated luminosity. Combining measurements of its area and mean surface brightness gives an estimated total B magnitude of 18.4 ± 0.5 for the integrated light. At the distance of the Centaurus cluster (taken here as $26.8 h^{-1} \text{Mpc}$), this is roughly $4h^{-2} \times 10^7 L_\odot$, corresponding to $8h^{-2} \times 10^7 M_\odot$ if we assume a mass-to-light ratio of $M/L_B = 2$.

3 N-BODY SIMULATIONS

3.1 Galaxy models

We shall use numerical simulations to investigate the possibility that the Centaurus arc is tidal debris from a gravitational interaction between a galaxy and one of the cD galaxies NGC 4696 or NGC 4709. Since the total stellar mass of the arc is just a few percent of the stellar mass of an L_* galaxy, it may have originated from a single dwarf spheroidal galaxy that was completely disrupted, or a bright spiral that had a small fraction of its disk stripped.

Given the wide parameter space to explore in both galaxy morphologies and orbital properties, we shall limit our choice of models to three; dwarf spheroidals, high surface brightness spirals and low surface brightness spirals. Elliptical galaxies are simply too centrally concentrated to loose a great deal of stellar mass. Even if a particularly strong tidal

shock unbound some stars, they would not occupy a narrow region of phase space required to produce a feature $\lesssim 2$ kpc across; tidal features have similar widths as the stellar system they originate from (Moore & Davis 1994).

If the Centaurus arc is tidal debris, then its position next to the cluster centre suggests that the potential of one of the massive central cD galaxies was responsible for the disruption. However, we can't rule out the possibility that the encounter took place further from the cluster centre and we are just observing the debris passing pericentre. Rather than treat the full cluster potential and its substructure, we shall model the cD galaxy as a single truncated isothermal dark matter halo with a moderate core radius of 50 kpc (see Figure 4(a)). The dark matter particles that represent the cluster potential have a mass $\sim 10^{10} M_\odot$ and softening of 20 kpc. We discuss the effects of a clumpy potential in Section 5.

The model galaxies are constructed using the techniques developed by Hernquist (1989). The spheroidal galaxy is constructed as a single stellar system, with a mass distribution shown in Figure 4(b). This is a truncated isothermal distribution of stars with a core radius of 2 kpc, and total mass within 20 kpc of $1.73 \times 10^{11} M_\odot$. This system would have a luminosity $\sim 2\% L_*$, therefore we must disrupt the entire galaxy in order to explain the arc. Dwarf spheroidals most probably result from harassed Sc-Sd galaxies, however, they are also the most common type of galaxy in clusters so it is possible that some of these systems are further disrupted by subsequent strong tidal encounters.

The low surface brightness (LSB) galaxy is modelled on a scaled version of UGC 128 (de Blok & McGaugh, 1998), using an exponential stellar disk with scale length $r_d = 10$ kpc and a dark halo with core radius set equal to the disk scale length. Within 3 disk scale lengths, the ratio of dark matter to stars is ~ 4.6 .

A characteristic of LSB galaxies is that they have slowly rising rotation curves, indicating that the central regions have almost uniform density. Therefore the central dynamical time-scales remain constant throughout the inner disk and an encounter that is impulsive at the core radius will be impulsive throughout the disk. For this reason, our pre-suspicion was that the LSB galaxy would be the most likely candidate for producing tidal debris most similar to the Centaurus arc.

The high surface brightness (HSB) galaxy is similar to the LSB galaxy, except that the disk and halo scale lengths are reduced by a factor of two and we include a bulge with mass $0.25 M_{disk}$ such that the rotation curve is flat over the central region (Figure 4(c)). Within 3 disk scale lengths the ratio of dark matter to stars is ~ 1.09 .

Both the LSB and HSB disks have scale height $r_z = 0.1r_d$ and are stable with a Toomre parameter $Q = 1.5$. The galaxies have modified isothermal dark matter halos with core radii set equal to r_d . Although both these galaxies have different internal mass distributions, they both have the same total luminosity and their rotation curves both peak at 200 km s^{-1} , therefore they both lie at the same point on the Tully-Fisher relation. We use 20,000 star particles in the disk and dark matter halo of the HSB galaxy and twice as many within the LSB galaxy. The softening lengths for these galaxies are set equal to $0.15r_d$ for the star particles

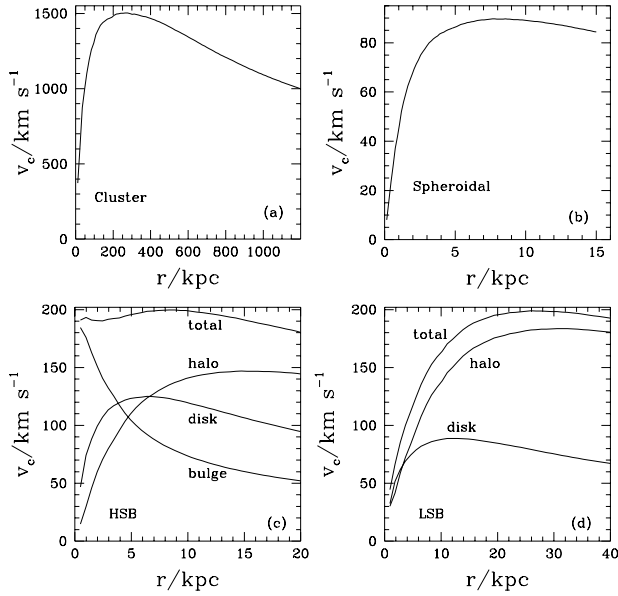


Figure 4. The rotation curves $\propto \sqrt{M/r}$ of (a) the cluster, (b) the spheroidal galaxy, (c) the HSB galaxy and (d) the LSB galaxy. The contribution to the rotation curve from the different components of the spiral galaxies are indicated.

and $0.7r_d$ for the halo particles. When we simulate the galaxies in isolation they are stable and remain in equilibrium.

To evolve the model galaxies in orbit through the cluster potential we use the parallel treecode “PKDGRAV” (Stadel *et al*, in preparation). It has an open ended variable timestep criteria based upon the local acceleration (Quinn *et al* 1997) and uses a spline force softening that is completely Newtonian at twice the quoted softening lengths.

3.2 Orbits

Fixing the orbit in the x-y plane we explore a range of orbital eccentricities, from completely radial to apo:peri=2:1. The more radial the orbit, the stronger the tidal shock and more material will be stripped. However, if the orbit is too radial, the stream may fan out as seen in the simulations of Weil, Bland-Hawthorn & Malin (1997) and will not produce a long thin tail of stars. We set the starting position at 1000 kpc for every run and vary the components of velocity using combinations of the following values:

$$\begin{aligned} v_x &= 0, 100, 200, 300, 400, 500 \\ v_y &= 0, 100, 200, 300, 400, 500 \end{aligned}$$

thus we explore a total of 25 orbits and choose the orbit that produced the longest and thinnest tidal debris. We evolve all the runs for 5 Gyr, about two orbital times for this configuration. From these trial runs we found that this was an orbit with $v_x = 400 \text{ km s}^{-1}$ $v_y = 300 \text{ km s}^{-1}$, which leads to an 8 : 1 orbit, *i.e.*: apocentric and pericentric distances of 1000 kpc and 120 kpc respectively. The velocity at pericentre is $\sim 3000 \text{ km s}^{-1}$. Note that the impact parameter past the centre of the potential and the velocity at pericentre determine the strength of the impulsive shock. The starting

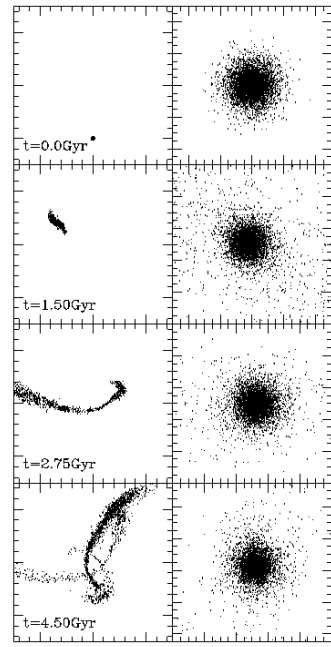


Figure 5. The evolution of the spheroidal galaxy on an orbit with apo:peri=8 : 1. The left hand panels show an area of 3000^2 kpc centred on the cluster potential, while the right hand side is a close-up view (100 kpc on each side) of the centre of the orbiting galaxy. Note that for clarity we plot just 1/5th of the star particles, projected onto the orbital plane and the cluster particles are not plotted to avoid confusion.

position and initial velocity could be varied to give a similar impact geometry.

Halos within clusters that form in a hierarchical universe have orbits that are close to isotropic (Ghigna *et al* 1998); circular orbits are rare and radial orbits are common. Ghigna *et al* (1998) find that 20% of all orbits have apo:peri ratios of at least 10 : 1, therefore the orbit that we have selected as optimum for producing narrow streams of tidal debris, is in fact a typical orbit for a cluster galaxy.

Note that the galaxies are constructed such that their halos extend well beyond the tidal radius, r_t , that would be imposed by the cluster potential at 120 kpc. Using the relation $r_t \sim r_{peri} * v_c(\text{galaxy})/v_c(\text{cluster})$, the tidal radii of our models on a circular orbit at 120 kpc would be 8 kpc for the spheroidal and 13 kpc for the spirals. However, the bulk of the stars orbit within these radii, therefore we rely on the impulsive shock as the galaxies move rapidly past pericentre to strip the stars from the central regions.

In Figure 5 we plot snapshots of the spheroidal system at four different epochs. As the galaxy moves in its orbit, most of the halo particles get stripped away, as is apparent from the left hand plots, but upon close examination of the central region we see that most of the material is still bound. After ~ 2.5 Gyr, the stripped stars form long arc like features, but these are not as thin or as bright as that observed within Centaurus.

The orbits of the spiral galaxies have an extra degree of freedom, namely the orientation of the disk as the galaxy moves past pericentre. We shall consider the extreme cases of a disk that is either counter-rotating or co-rotating such that the disk lies in the orbital plane. Figure 6 shows the

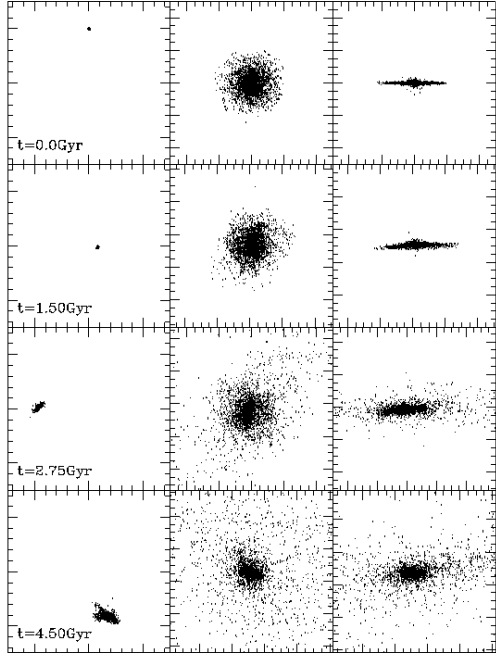


Figure 6. The evolution of the HSB galaxy in a counter-rotating orbit. Right panels correspond to a face on and edge on view of the galaxy within a box of 100 kpc on each side, the left panel is the full view of the orbit in a box of 3000^2 kpc centered on the cluster. Cluster particles are not shown.

evolution of the HSB galaxy counter-rotating with respect to the orbital direction past pericentre. The first tidal shock occurs after a Gyr, yet even after 1.5 Gyr the disk does not appear to be highly perturbed. After 2.75 Gyrs most of the stars are still orbiting within a thick disk, yet no spiral features remain. At this time the galaxy resembles an S0!

Continued heating of the galaxy after a total of 4 passages past pericentre has not removed a great deal of stars from the galaxy, yet a flattened stellar configuration is only just apparent at late times. By the final time 30% of the stars have been unbound from the disk, however, the stripped stars orbit close to the galaxy and throughout the simulation we never observe long, thin tidal features.

The LSB galaxy on an identical orbit as the HSB galaxy is shown in Figure 7. The evolution proceeds in a similar fashion, yet the inner disk is clearly more perturbed and by the final time, no trace of the original disk structure is apparent. This time, after 2.7 Gyrs 52% of the stars are unbound, yet again we do not find any features that resemble the Centaurus arc, either in dimension or surface brightness.

We now change the direction of the orbit through the cluster potential such that the disk is co-rotating with the galaxy's direction past pericentre. After just 1.5 Gyrs, the morphology of the HSB galaxy shown in Figure 8 has been dramatically altered. Already, most of the disk structure has been destroyed, and the stellar distribution has been significantly heated. However, the most significant change occurs in the morphology of the tidal debris. After 2.75 Gyrs, we start to observe long thin tidal tails of stars that have been symmetrically torn from the disk. Continued heating of the galaxy removes more material from the disk and the tidal tails stretch out further along the orbital path of the galaxy.

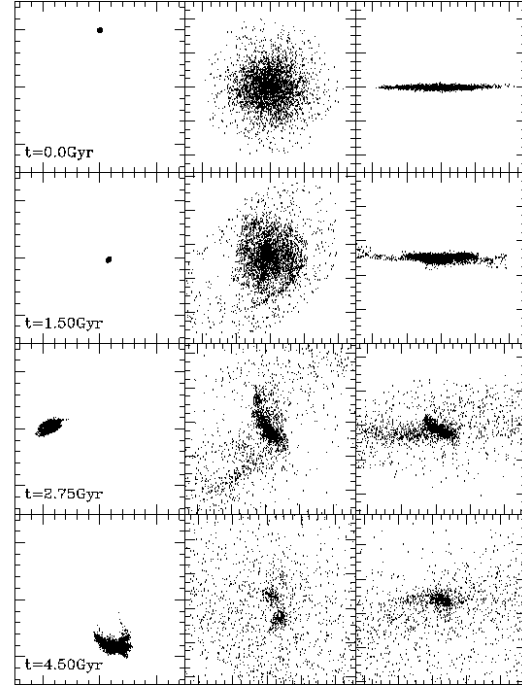


Figure 7. The evolution of the LSB galaxy on a counter-rotating orbit. The left panels show the entire orbit centered on the cluster potential in a 3000^2 kpc box. The two right hand panels measure 100 kpc on the side and correspond to a close up view of the galaxy: face on, centre panel and edge on in the right panel.

The LSB galaxy on a co-rotating orbit, shown in Figure 9, is almost completely destroyed by the tidal forces. After 2.75 Gyrs more than 57% of the disk has been removed and forms long thin tidal tails that stretch for several hundred kpc on either side of the galaxy. By the end of the simulation, just a few percent of the stars remain bound in a configuration that resembles a dwarf spheroidal, with an exponential surface brightness distribution.

The full view of the LSB and HSB co-rotating orbits look very similar; both produce long thin tidal tails. Upon close inspection it is evident that there are particular instances where long “arc like” features are more apparent. The best of these typically occur ~ 2.7 Gyrs after the galaxy enters the cluster, a time when the debris stripped at first passage past pericentre is orbiting past the cluster centre the second time. It is also apparent from Figures 8 and 9, that the debris has the narrowest dimension and would be most luminous as it is passing pericentre. At this point, the orbits of the stars bunch up because they are in the deepest part of the potential. It is this section of the tidal debris that we associate with the Centaurus arc that also lies close to the centre of the cluster potential.

Can we distinguish between these two possibilities? At time $t = 2.75$ Gyrs we extract a 300 kpc length of the stellar debris that is just approaching pericentre. We then project the data and create smoothed density surface density plots and overlay contours of constant surface density.

These density maps are plotted in Figure 10 and demonstrate that debris from both HSB and LSB galaxies can create long ($\gtrsim 200$ kpc) and thin ($\lesssim 8$ kpc) diffuse arc-like features. These have similar morphological appearance to the

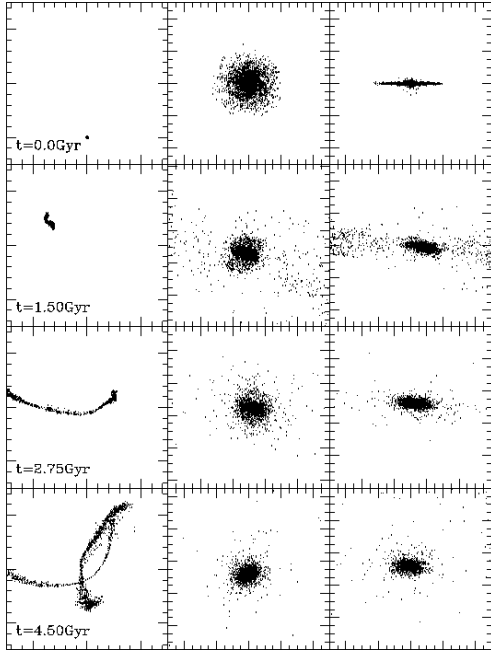


Figure 8. As Figure 6, except the HSB galaxy has been placed on a co-rotating orbit.

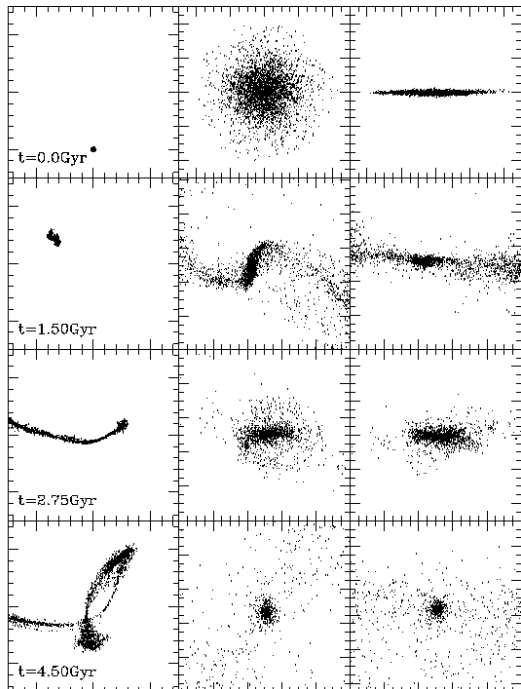


Figure 9. As Figure 7, except the LSB galaxy has been placed on a co-rotating orbit.

Centaurus arc yet differ in their overall surface brightness. The central surface brightness of the inner contour of the LSB galaxy is $\mu_B = 27.85 \text{ arcsec}^{-2}$, while for the HSB it is $\mu_B = 28.33 \text{ arcsec}^{-2}$. For this conversion we have assumed a mass to light ratio of $M/L_B = 2$.

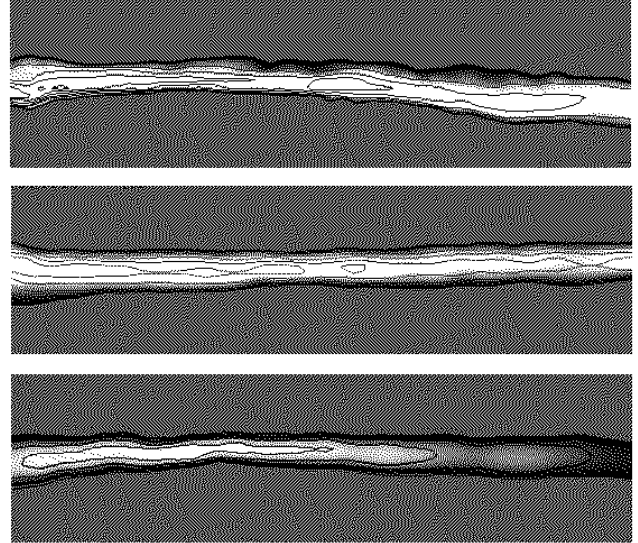


Figure 10. Projected density maps of a region 300 kpc by 200 kpc around the thin arc-like structures formed by the LSB and HSB models. The top panel corresponds to the LSB feature viewed at an angle of 15° from edge on and the middle panel is an edge on view of the same. The bottom panel is an edge on view of the HSB debris. The contours are curves of constant surface brightness in the range $27 - 31$ for the LSB model and $28 - 31$ for the HSB (in blue magnitudes per arcsec^2).

4 DISCUSSION

We now have the necessary results to refine the possible galaxy type and orbital geometry that could have produced the Centaurus arc. Each model was able to produce long arc-like features, but in every case major differences distinguish them.

For the spheroidal model, long streams of debris are obtained, but they are over 3 magnitudes too faint to explain the Centaurus arc. Even after several passages past pericentre, most of the material remains bound to the galaxy. We would require the entire spheroidal to be disrupted into a single smooth stream of length ~ 100 kpc in order to explain this feature. We were unable to achieve this.

Spiral galaxies can have luminosities much larger than the fainter spheroidal systems, therefore a smaller fraction of their stars can be stripped to form observable debris. We find a strong dependence upon the amount of material stripped and its subsequent orbital path through the cluster, with the relative motion of the disk stars as the system moves past pericentre. A larger fraction of stars were stripped from disks that are co-rotating with their orbit, and the stripped stars formed long narrow streams that resembled the Centaurus arc.

We can understand why this happens by considering the relevant dynamical time-scales. The impulsive shock occurs on a time-scale $t_o = 2r_p/v_i$ Gyrs, where the impact velocity of the galaxy is $v_i = 3000 \text{ km s}^{-1}$ as it moves past pericentre $r_p = 120$ kpc. We can compare this time-scale with the time it takes for the disk stars to make half a revolution within the core radius of the galaxy, r_{core} , $t_i = \pi r_{\text{core}}/v_c$, where $v_c = 200 \text{ km s}^{-1}$. For the particular galaxy and orbit

simulated here, $t_i \sim t_o = 0.1$ Gyrs. If the disk is co-rotating, then the encounter occurs at a resonance, whereas a counter-rotating orbit gives time for the central disk stars to respond adiabatically to the encounter.

The LSB is particularly affected by the resonance since the dynamical time within the core radius is constant (due to the constant density of the mass distribution within a disk scale length). Therefore the entire disk is affected by the tidal shock. The HSB galaxy also has a resonance, but only at a single annuli in the disk since the dynamical time increases linearly with radius. This explains why both the disk galaxies produced long thin tails of debris, but those from the LSB galaxy are much brighter since it lost a great deal more mass with only 17% remaining bound.

Our simulations showed that the orbits of the stripped stars move closer together as they move through pericentre. This creates the appearance of a “standing wave” near the cluster centre, where the surface brightness of the debris is significantly enhanced.

We can understand why the orbits bunch together near pericentre and make a rough quantitative estimate of the enhancement in surface brightness as follows: Consider two stars in circular orbits near the cluster centre at distances r_{a1} and r_{a2} , separated by a small radial distance Δr_a . What happens to the separation of the particles as we move the orbits further out into the cluster, but preserve the small energy difference between the two particles? Now the particles orbit at distances r_{p1} and r_{p2} , this time separated by Δr_p .

The total energy of each orbit (E_i) is conserved and equal to $E_i = K_i + \Phi_i$ Where K_i is the kinetic energy term for each orbit and $\Phi_i = 2\sigma^2 \ln \frac{r_i}{R}$ [†] its corresponding potential energy. Because we are dealing with an isothermal potential, all circular orbits have the same kinetic energy, therefore the difference in total energy for each pair of orbits is given by:

$$|\Delta E_A| = |\Phi_A| = |2\sigma^2 \ln(r_{a2}/r_{a1})|$$

$$|\Delta E_P| = |\Phi_P| = |2\sigma^2 \ln(r_{p2}/r_{p1})|$$

If the energy difference of both orbits is the same then

$$|\Delta E_A| = |\Delta E_B|$$

$$\ln(r_{a2}/r_{a1}) = \ln(r_{p2}/r_{p1})$$

therefore we can write

$$r_{a2}/r_{a1} = r_{p2}/r_{p1},$$

which leads to

$$\Delta r_a = (r_{a1}/r_{p1})\Delta r_p.$$

Thus for a given energy difference; orbits tend to get closer together as they move towards the central regions of the potential. For an orbit with apo:peri of 10:1, the enhancement of the surface brightness the tidal stream will be roughly a factor of 10 at pericentre.

Further support for stellar debris of a galactic origin can be found by considering the colours of the Centaurus arc. In Table 2 we give typical colour differences for galaxies of different morphologies across the Hubble diagram (Frei &

[†] Note that we have use a *truncated* isothermal spherical potential where σ is the constant velocity dispersion and R is the truncation radius.

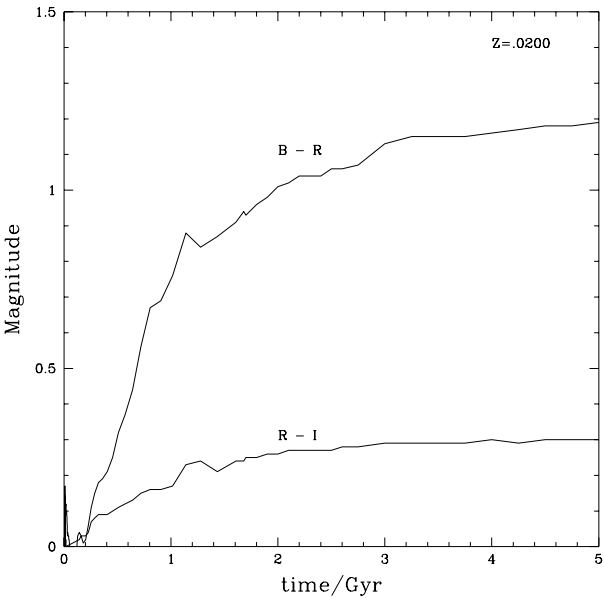


Figure 11. Colour fading as a function of time for B-R and R-I colour differences.

	Ellipticals	Sab's	Scd's	LSB
B-R	1.48	1.04	0.86	0.78
R-I	0.57	0.57	0.43	0.49

Table 2. Typical colour differences for different galaxy morphologies.

Gunn 1994; de Blok *et al* 1995). Once the stars are removed from the galaxy, star formation will be abruptly halted and the stars will fade in a predictable manner. Figure 11 shows how the colour indices fade with time for a given stellar population with known metallicity and IMF (Bruzual & Charlot).

The tidal tails match the appearance of the Centaurus arc ~ 1 Gyr after being stripped from the model galaxies. i.e. the time since the first passage past pericenter. After a Gyr, the amount of fading will be 0.77 and 0.17 for B-R and R-I, respectively. We now reconsider the observed values for the arc (see Table 1). We add a further correction for galactic dust reddening using the data of Burstein & Heiles (1982) and Schlegel *et al* (1998); this brings the values of the colours to:

$$B - R = 1.52 \pm 0.14$$

$$R - I = 0.27 \pm 0.23$$

If we take into account the amount of fading over one Gyr, then the initial stellar colours of the stars in the arc would have been $B - R = 0.75$ and $R - I = 0.10$. These colours, within the uncertainties, are consistent with late type spirals and LSB disk galaxies, providing further support for our model.

5 CONCLUSIONS

We present deep photographic and CCD observations of a spectacular arc of diffuse light in the Centaurus cluster. This feature is remarkable given its length and narrowness, $\sim 12 \text{ arcmin} \equiv 120h^{-1} \text{ kpc}$ long and $\sim 10 \text{ arcsec} \equiv 2h^{-1} \text{ kpc}$ wide. The arc is diffuse with no apparent structure and its colours indicate that it is made of stars. The estimated total mass from its integrated luminosity is $\sim 8h^{-2} \times 10^7 M_\odot$ and its surface brightness (in mag arcsec^{-2}) is $\mu_B = 27.8$; $\mu_R = 26.1$; in the R band and $\mu_I = 25.7$, in the I band. Several possible scenarios for its origin, including foreground reflection nebulae, gravitational lensing or a radio jet, are rejected in favor of a gravitational tidal interaction that created an arc of stellar debris. A second feature with similar morphology is also revealed within the central region of the Coma cluster.

We used numerical simulations to investigate the response of galaxies of different morphologies to tidal shocks as they pass pericentre in a cluster potential. Spheroidal, HSB and LSB galaxy models were evolved on orbits through a smooth cluster potential. From many different trial orbits, a galaxy moving through the cluster within apocentre:pericentre of 8:1 produced the narrowest, longest and brightest tidal tails. This orbit is typical for galaxies orbiting in clusters that form within hierarchical clustering models (Ghigna *et al* 1998).

Even though the parameter space is large, we can effectively eliminate spheroidal or high surface brightness spiral galaxies from the possible list of harassed galaxies. The spheroidal galaxy loses only about 15% of its central mass to the cluster and the features formed are wide and extremely diffuse and would not be observable. In the case of the HSB model, only about 30% of its stellar mass is lost during the simulation, and although long thin arc like debris are produced they are also fainter than the Centaurus arc.

The only models that can produce tidal features this long and thin are disk galaxies. Moreover, in order to reproduce the surface brightness of the Centaurus feature, the galaxy must be a massive LSB galaxy with a luminosity close to L_* . In addition to the well defined morphology, we are also forced to use orbits that place the disk in the global orbital plane and the disk must be rotating in a prograde sense, co-rotating with the orbital path past pericentre. This encounter geometry produces the maximum resonant stripping of disk material - almost ninety percent of the disk is removed yet just a few percent constitutes the luminous part of the debris that we associate with the Centaurus arc. Although the tidal debris from a single galaxy can span the entire cluster, as the stars move past pericentre, their orbits move closer together and the streams would appear brighter.

We note that there is a way to confirm the galactic origin of the Centaurus arc. By taking images along its length using different filters, (*e.g.* OIII or H α) as discussed in Feldmeier *et al* (1997), one would expect to find an over abundance of planetary nebulae at similar redshifts to NGC4709; thus confirming the stellar nature and formation mechanism.

The tidal tails of stellar debris follow the progenitor galaxies orbit through the cluster and stretch for several Mpc. The coherent length of structure in the diffuse light will be much shorter than this since the real cluster potential is far from smooth. The other cluster galaxies will disrupt

the tidal tails, “chopping” them into pieces. On average, each galaxy in a cluster experiences a close encounter with one of its massive cluster companions at a rate of one per Gyr, thus short sections of narrow features may survive for a crossing time. However, even deeper images of the feature may reveal the arc extending further from the cluster centre. Somewhere along the tidal tails lies the remnant spheroidal galaxy surrounded by a cloud of diffuse light that closely resembles the feature reported by Trentham & Mobasher (1997). Thus galaxy harassment can be used, in general, to explain the diffuse light within clusters.

ACKNOWLEDGMENTS

Carlos Calcáneo-Roldán would like to thank the People of México for their generous support, through a grant by CONACyT, which allows him to continue his research. Ben Moore is a Royal Society research fellow. Computations were carried out as part of the Virgo consortium.

REFERENCES

Arnaboldi, M., Freeman, K. C., Mendez, R. H., Capaccioli, M., Ciardullo, R., Ford, H., Gerhard, O., Hui, X., Jacoby, G. H., Kudritzki, R. P. & Quinn, P. J., 1996, ApJ, 472, 145.

Bernstein, G.M., Nichol, R.C., Tyson, J.A., Ulmer, M.P. & Wittman D., 1995, AJ, 110, 1507.

Bruzual, A. G. & Charlot, S., 1993, ApJ, 405, 538.

Bruzual, A. G. & Charlot, S., 1998, in preparation.

Burstein, D. & Heiles, C., 1982, AJ, 87, 1165.

Conselice, C. J. & Gallagher, J. S. 1999, AJ, in press (astro-ph/9809390).

Cousins, A. W. J., 1981, SAAO Circulars, 1(6), 4.

de Blok, W. J. G. & McGaugh, S. S., 1998, ApJ, 499, 66.

de Blok, W. J. G., van der Hulst, J. M. & Bothun, G. D., 1995, MNRAS, 274, 235.

de Vaucouleurs, G., 1960, ApJ, 131, 585.

Feldmeier, J. J., Ciardullo, R. & Jacoby, G. H., 1997, ApJ, 479, 231.

Ferguson, H. C., Tanvir, N. R. & von Hippel, T., 1998, Nature, 391, 461.

Frei, Z. & Gunn, J. E., 1994, AJ, 108, 1476.

Ghigna, S., Moore, B., Governato, F., Lake, G., Quinn, T. & Stadel, J., 1998, MNRAS, 300, 146.

Gunn, J. E., 1969, BAAS, 1, 191.

Hernquist, L. & Katz, N., 1989, ApJS, 70, 419.

Malin, D. F., 1978, Nature, 276, 591.

Malin, D. F., 1981, Phot. Sci., 29, 199.

Merritt, D., 1984, AJ, 276, 26.

Mihos, J. C., McGaugh, S. S. & de Blok, W. J. G., 1997, ApJ Lett, 477, L79.

Moles, M., Garcia-Pelayo, J. M., Masegosa, J. & Aparicio, A., 1985, ApJS, 58, 255.

Moore, B. & Davis, M., 1994 MNRAS, 270, 209.

Moore, B., Katz, N., Lake, G., Dressler, A., & Oemler, A. J., 1996, Nature, 379, 613.

Moore, B., Lake, G. & Katz, N., 1998, ApJ, 495, 139.

Moore, B., Governato, F., Quinn, T., Stadel, J. & Lake, G., 1998, ApJ Lett., 499, L5.

Quinn, T., Katz, N., Stadel, J. & Lake, G., 1997, submitted to ApJ, (astro-ph/9710043).

Scheick, X. & Kuhn, J. R., 1994, ApJ, 423, 566.

Schlegel, D. J., Finkbeiner, D. P., Davis, M., 1998, ApJ, 500, 525.

Tarenghi, M., 1981, in Optical Jets in Galaxies, ESA SP-162, 145.

Theuns, T. & Warren, S. J., 1996, MNRAS, 284, L11.

Thuan, T. X. & Kormendy, J., 1977, PASP, 89, 466.

Trentham, N. & Mobasher, B., 1998, MNRAS, 293, 53.

Tyson, J.A. & Fischer, P., 1995, ApJ Lett., 446, L55.

Uson, J. M., Boughn, S. P. & Kuhn, J. R., 1991, ApJ, 369, 46.

Vilchez-Gómez, R., Pelló, R. & Sanahuja, B., 1994, A&A, 283, 37.

Weil, M.L., Bland-Hawthorn, J. & Malin, D.F., 1997, ApJ, 490, 664.

Zwicky, F., 1951, PASP, 63, 61.

This figure "fig1.jpg" is available in "jpg" format from:

<http://arxiv.org/ps/astro-ph/9811450v1>

This figure "fig2.jpg" is available in "jpg" format from:

<http://arxiv.org/ps/astro-ph/9811450v1>